

## Optical band gap of $\text{NpO}_2$ and $\text{PuO}_2$ from optical absorbance of epitaxial films

T. Mark McCleskey,<sup>1,a)</sup> Eve Bauer,<sup>1</sup> Quanxi Jia,<sup>1</sup> Anthony K. Burrell,<sup>2</sup> Brian L. Scott,<sup>1</sup> Steven D. Conradson,<sup>1</sup> Alex Mueller,<sup>1</sup> Lindsay Roy,<sup>3</sup> Xiaodong Wen,<sup>1</sup> Gustavo E. Scuseria,<sup>4</sup> and Richard L. Martin<sup>1</sup>

<sup>1</sup>MPA-MC, Mail Stop J514, Los Alamos National Laboratory, Los Alamos, New Mexico 87545, USA

<sup>2</sup>Argonne National Laboratory, Argonne, Illinois 60439, USA

<sup>3</sup>Savannah River National Laboratory, Savannah River Site, Aiken, South Carolina 29808, USA

<sup>4</sup>Department of Chemistry, Rice University, Houston, Texas 77005, USA

(Received 19 June 2012; accepted 1 November 2012; published online 4 January 2013)

We report a solution based synthesis of epitaxial thin films of neptunium oxide and plutonium oxide. Actinides represent a challenge to first principle calculations due to features that arise from  $f$  orbital interactions. Conventional semi-local density functional theory predicts  $\text{NpO}_2$  and  $\text{PuO}_2$  to be metallic, when they are well known insulators. Improvements in theory are dependent on comparison with accurate measurements of material properties, which in turn demand high-quality samples. The high melting point of actinide oxides and their inherent radioactivity makes single crystal and epitaxial film formation challenging. We report on the preparation of high quality epitaxial actinide films. The films have been characterized through a combination of X-ray diffraction and X-ray absorption fine structure (XANES and EXAFS) measurements. We report band gaps of  $2.80 \pm 0.1$  eV and  $2.85 \pm 0.1$  eV at room temperature for  $\text{PuO}_2$  and  $\text{NpO}_2$ , respectively, and compare our measurements with state-of-the-art calculations. © 2013 American Institute of Physics. [<http://dx.doi.org/10.1063/1.4772595>]

### INTRODUCTION

The actinide dioxides  $\text{PuO}_2$  and  $\text{NpO}_2$  are important nuclear fuel materials. Today, fuel rods are taken out of service at 5% burn up or less. In order to make more effective use of the fuel, we need to understand how thermal conductivity changes over time in a fundamental manner as the composition of the fuel rod changes due to the emergence of fission products over time. Especially important is a better understanding of Pu oxide and Pu/U oxide mixtures to make effective use of new MOX fuels. From a theoretical perspective, prediction of complex properties such as thermal transport begins with a solid understanding of orbital interactions and band gap formation. We have for the first time performed the direct optical measurement of the band gap for  $\text{PuO}_2$  and  $\text{NpO}_2$ . Theoretical calculations can now be benchmarked on these fundamental measurements and then applied to mixtures.

Actinides represent a tremendous challenge to first principle calculations due to the complicating features that arise from  $f$  orbital interactions. The strong correlations associated with  $f$  orbital electrons are exemplified by the Mott insulator  $\text{UO}_2$ . The workhorse of electronic structure approximations for materials, the local density approximation (LDA) of density functional theory (DFT), predicts  $\text{UO}_2$  to be a ferromagnetic metal. In fact, it is an antiferromagnetic insulator with a band gap of 2.3 eV. Successive generations of semi-local DFT approximations, the generalized gradient approximation (GGA), and meta-GGA approximation, do no better.<sup>1</sup> These approximations contain an inaccurate treatment of the

self-interaction term, leading to an overestimation of electron repulsion. Three approaches have been used to address this problematic term: a fourth generation functional, hybrid DFT;<sup>2</sup> the self-interaction correction (SIC);<sup>3</sup> the DFT + U technique.<sup>4</sup> These approaches predict the correct ground state, insulating properties, and gap for  $\text{UO}_2$ , although the most recent SIC calculations yield a metal for  $\text{UO}_2$ .<sup>3</sup> The DFT + U approximation replaces the atomic electron repulsion terms among the  $f$  electrons with a parameter U; as U is varied from 0 to 6, the behavior of  $\text{NpO}_2$  goes from metallic to a band gap  $> 3.0$  eV. An embedded cluster approach, dynamic mean-field theory (DMFT), builds upon a DFT + U base and has also met with some success in yielding insulators as opposed to metals in these complicated materials, although the results are once again dictated by the choice of the parameter U.<sup>5,6</sup>

Verification of these calculations for predicting the properties of transuranic materials requires high quality solids such as single crystals and epitaxial films. Experimental work is complicated by the radioactivity that makes chemical vapor deposition processes challenging from a safety perspective and by the recalcitrant nature of the oxides.  $\text{PuO}_2$  melts at 2400 °C and  $\text{NpO}_2$  melts at 2547 °C, making single crystal formation through a melt process difficult. The reports of  $\text{PuO}_2$  single crystals are limited to two examples of crystal  $\text{PuO}_2$  formation from a flux comprising a mixture of  $\text{Li}_2\text{O}$  and  $\text{MoO}_3$  and the color of the crystals is reported as black in contrast to the olive green color of bulk  $\text{PuO}_2$  powders.<sup>7–9</sup> Most references to a band gap for  $\text{PuO}_2$  cite the McNeilly paper from 1962 which reports an activation barrier to electronic conduction of 1.8 eV.<sup>10</sup> For neptunium oxide, there are many more reports of single crystals,<sup>11–13</sup> but

<sup>a)</sup>Author to whom correspondence should be addressed. Electronic mail: tmark@lanl.gov. Telephone: 505-667-5636. Fax: 505-667-9905.

once again the only measurement of the band gap is from a measurement of the activation barrier to electronic conduction.<sup>14</sup> No direct measurement of the optical band gap has been performed for either  $\text{NpO}_2$  or  $\text{PuO}_2$ . We report on a solution route to yield high quality epitaxial films of actinide dioxides including  $\text{PuO}_2$  and  $\text{NpO}_2$  with rocking curves of  $0.07^\circ$ . The films have been characterized through a combination of X-ray diffraction (XRD) and X-ray absorption near edge structure (XANES) measurements to verify the epitaxial nature of the films and the oxidation state of the Pu. The thin epitaxial films enable the direct measurement of the optical band gap.

## RESULTS AND DISCUSSION

We have prepared thin epitaxial films of  $\text{PuO}_2$  and  $\text{NpO}_2$  using the solution based process of polymer assisted deposition (PAD). The PAD process was developed at Los Alamos National Laboratory and has been previously reported to make high quality epitaxial films of oxides, carbides, and nitrides.<sup>15–17</sup> For the transuranic materials, we modified the procedure slightly to avoid pressure filtration. Precursor solutions of metal-ethylenediaminetetraacetic acid (EDTA) complexes bound to the polymer polyethyleneimine (PEI) were prepared as homogeneous solutions with a pH near 5. The Np is a  $\text{Np(V)EDTA}$  complex based on visible absorption data and the Pu is the expected  $\text{Pu(IV)EDTA}$  complex.<sup>18,19</sup> The solutions were placed on single crystal substrates by spin coating  $30\ \mu\text{l}$  onto the surface of a  $1 \times 1\ \text{cm}$  substrate. The coated substrate was then annealed in a furnace to produce the final film. We have previously shown that PAD appears to be a bottom up growth technique and the lattice match to the substrate can have a significant effect on the crystal structure of resulting films.<sup>20,21</sup> For example,  $\text{UO}_2$  is obtained on an lanthanum aluminum oxide (LAO) substrate and  $\text{U}_3\text{O}_8$  is obtained on sapphire substrates even under identical annealing conditions. The hexagonal lattice of sapphire is well matched to the hexagonal  $\text{U}_3\text{O}_8$  lattice, while the  $\text{UO}_2$  lattice lines up well along the diagonal of the pseudo cubic LAO with only a 2% lattice mismatch.<sup>20</sup> In the case of neptunium, the effect of substrate on the thin film quality can be seen in Figure 1. Polycrystalline films of  $\text{NpO}_2$  were obtained on an LAO single crystal substrate (Figure 1(a)). Applying a buffer layer of  $\text{UO}_2$  on the LAO surface with subsequent coating of the Np solution leads to preferentially aligned films in which the 2 theta scans show only ( $h00$ ) reflections (Figure 1(b)). The (200) and (400) peaks are doublets comprising both  $\text{UO}_2$  and  $\text{NpO}_2$  reflections. Unfortunately, the buffer layer of  $\text{UO}_2$  complicates further measurements to determine the optical band gap and measure other optical properties such as refractive index. We also coated films onto YSZ. These films show excellent preferential alignment along ( $h00$ ) as evidenced by the XRD measurement (Figure 1(c)).

There is a slightly larger lattice mismatch for  $\text{NpO}_2$  with YSZ, than the diagonal alignment with LAO, but YSZ has advantages as a substrate in that there is only one type of termination and there is no phase change upon heating and cooling. LAO can terminate as lanthanum oxide or aluminum oxide and it undergoes a phase change from orthorhombic to

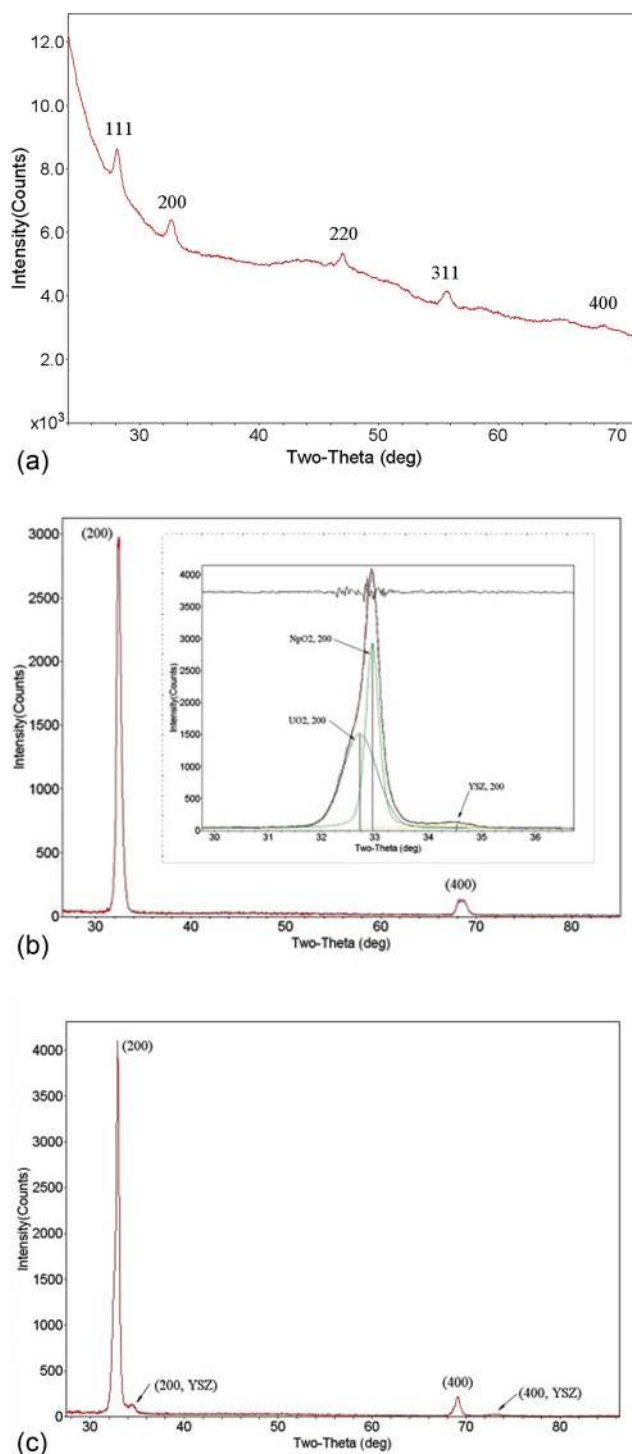


FIG. 1. (a) X-ray diffraction pattern showing polycrystalline film of  $\text{NpO}_2$  on LAO. (b) X-ray diffraction pattern of epitaxial film of  $\text{NpO}_2$  on a buffer layer of  $\text{UO}_2$  on LAO. Inset shows overlap of 200 peaks of  $\text{NpO}_2$  and  $\text{UO}_2$ . (c) X-ray diffraction pattern showing epitaxial thin films of  $\text{NpO}_2$  on YSZ.

cubic with slight lattice distortion during the thermal process, both of which can strain a thin film. High quality epitaxial films of both  $\text{NpO}_2$  and  $\text{PuO}_2$  were obtained on YSZ substrates. Rocking curve of the (200)  $\text{PuO}_2$  showed a  $0.07^\circ$  full width at half maximum (FWHM) that is approaching the single crystal substrate peak (Figure 2(a)).

$\text{UO}_2$  is known to become hypostoichiometric with  $\text{U}_3\text{O}_8$  as the thermodynamically stable species and  $\text{U(VI)}$  can be

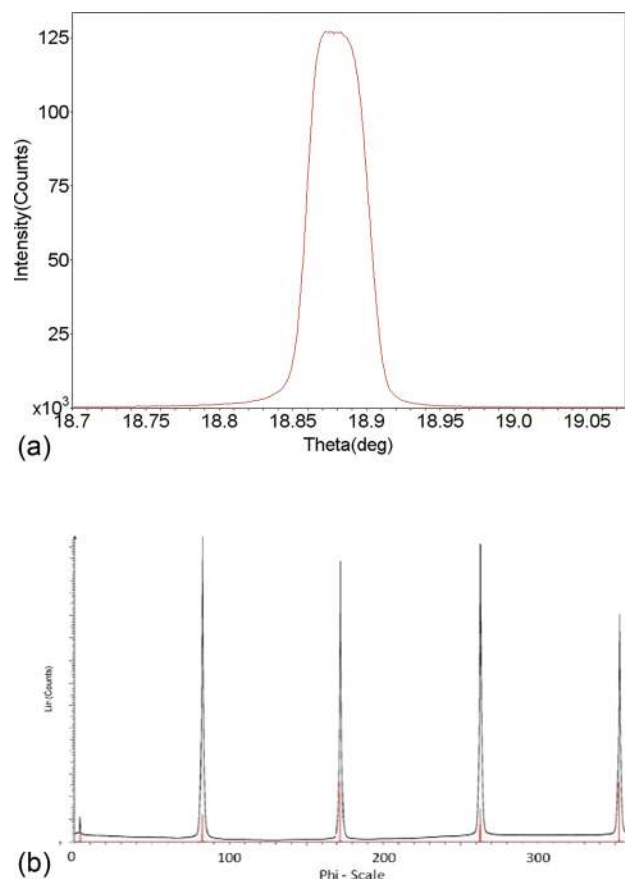


FIG. 2. (a) Rocking curve for the 200 reflection of  $\text{PuO}_2$  on YSZ. Alignment in plane is evidenced by the phi scans in (b). The  $\text{PuO}_2$  [100] is aligned along the substrate [100]. (b) Phi scans of the 220 reflection of  $\text{PuO}_2$  (black) on YSZ (red).

readily isolated as  $\text{UO}_3$ . As one goes across the periodic chart to Np and Pu, the trend is toward lower oxidation states. Np(V) oxidation is observed in  $\text{Np}_2\text{O}_5$  and  $\text{NpO}_2$  is favored thermodynamically.<sup>22</sup> Pu(III) is found in  $\text{Pu}_2\text{O}_3$  with  $\text{PuO}_2$  still being favored thermodynamically.<sup>23</sup> There have been recent reports on  $\text{PuO}_{2+x}$  species including evidence based on oxidation of single crystals based on O 1s X-ray absorption data.<sup>8,24,25</sup> To verify oxidation state and the degree of ordering of the films, we performed Pu  $L_3$  XAFS measurements. Pu XANES spectra are highly sensitive to reduction because of the large difference in energy between the III and IV valences.<sup>26</sup> The XANES of two separately prepared films overlay each other and the spectrum of high purity  $\text{PuO}_2$ , corroborating the reproducibility of the synthesis and the absence of significant amounts of Pu(III) as contaminants in the material (Figure 3(a)).

The larger amplitudes of the peaks could result from less saturation of the Ge detector system over the peak and/or less self absorption relative to the bulk sample that was ground by hand and is, therefore, composed of particles larger than the film thickness. The extended X-ray absorption fine structure (EXAFS) region of the spectrum complements XRD analysis because it receives population-weighted contributions from all of the components in the sample and not only the periodic ones. The relatively small amount of Pu in the film results in more noise at higher R values that makes it difficult to assess the longer range order as well as larger background residuals

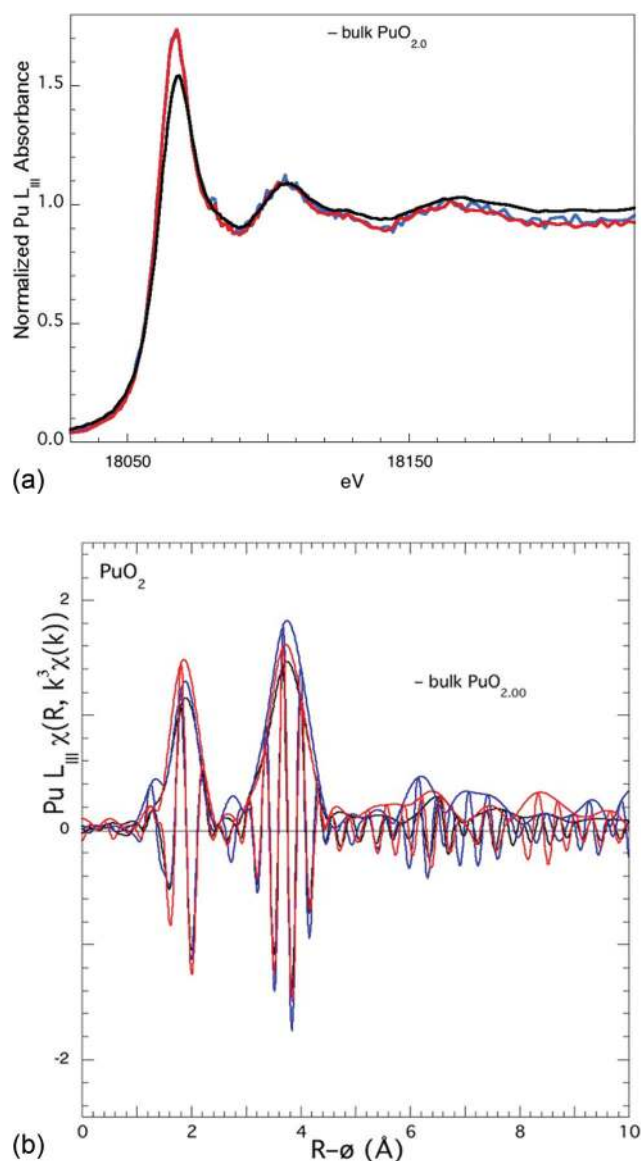


FIG. 3. (a) XANES of  $\text{PuO}_2$  powder (black) and two separately prepared  $\text{PuO}_2$  films (blue and red). (b) EXAFS of  $\text{PuO}_2$  powder (black) and thin films (blue and red).

as lower R shoulders on the nearest neighbor O contribution. It is, however, nevertheless clear that the peaks in  $\chi(R)$  at  $R = 1.8$  and  $3.8 \text{ \AA}$  that are the contributions of the primary nearest neighbor O and Pu shells are larger in amplitude than those from the bulk powder (Figure 3(b)). This indicates that the degree of ordering in these samples may be even higher than in that single phase powder. The XANES data clearly show Pu(IV) oxidation as compared to high quality samples of  $\text{PuO}_2$  powder.

One of the advantages of thin films over crystals is that they allow for the measurement of optical properties that can be difficult with thick samples. We performed measurements of the optical band gaps of both  $\text{PuO}_2$  and  $\text{NpO}_2$  at different film thicknesses by coating multiple times. The plots of  $(\epsilon^*h\nu)^2$  vs  $h\nu$ , used for direct band gap semiconductors, show linear fits at high energy with intercepts of the band gap at  $2.80$  and  $2.85 \pm 0.1 \text{ eV}$  for  $\text{PuO}_2$  (Figure 4) and  $\text{NpO}_2$ , respectively.

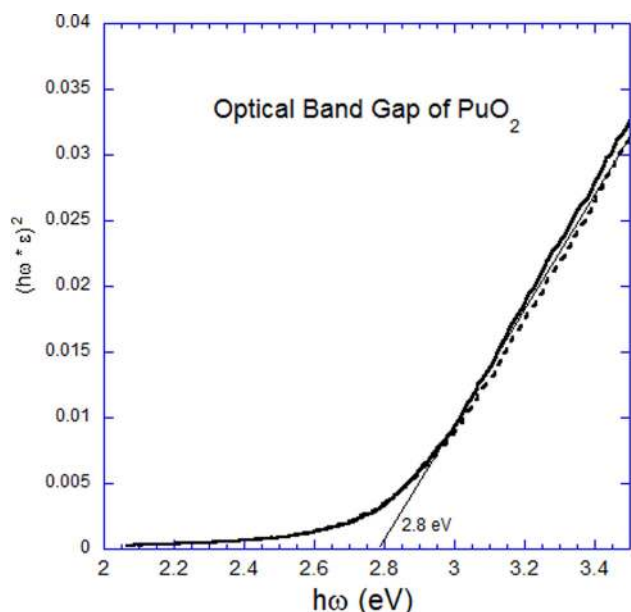


FIG. 4. Optical band gap of  $\text{PuO}_2$  based on absorption with 3 (solid line) and 5 (dashed line) coats of  $\text{PuO}_2$  on YSZ.

This is the first time that the optical band gaps of  $\text{PuO}_2$  and  $\text{NpO}_2$  have been measured and they differ significantly from the literature cited values of 1.8 eV and 0.4 eV for  $\text{PuO}_2$  and  $\text{NpO}_2$ , respectively.<sup>10,14</sup> In the past,  $\text{UO}_2$  single crystal has been polished to allow for accurate optical band gap measurement,<sup>27</sup> but no such work has been done on the  $\text{PuO}_2$  or  $\text{NpO}_2$  single crystals.

Previous literature reports have measured the activation energy for electronic conduction using pressed powders. This is done by taking resistivity measurements as a function of temperature. In the case of  $\text{PuO}_2$ , McNeilly fit the data to a straight line at temperatures greater than 200 °C with the measurements done under vacuum.<sup>10</sup> Activation barriers to electronic conduction can be significantly lower than the band gap and are very sensitive to defects and vacancies. For example, copper selenide thin films with an optical band gap of 2.03 eV have been reported to have an activation barrier to electronic conduction as low as 0.20 eV.<sup>28</sup> The value of 1.8 eV measurement from McNeilly's work has been referenced as a band gap value and has become a benchmark for all theoretical works used to model  $\text{PuO}_2$ . In the report, it states "The lack of single crystal specimens also places somewhat of a limit on the interpretation of results."<sup>10</sup> As the author notes,  $\text{PuO}_2$  has a tendency to lose oxygen to form sub-stoichiometric oxides.<sup>9</sup> For the  $\text{PuO}_{2.0}$  sample that was measured, the value of 1.8 eV was obtained from a fit of data from 200 to 1000 °C. Below 200 °C, the data fall far below the extrapolated line. The data from room temperature to 200 °C are nearly linear with a slope that yields a barrier to electronic conduction of approximately 3 eV. In the case of  $\text{NpO}_2$ , measurements were done over a temperature range of 150–300 K, and the data do not fit a straight line over the entire energy range. Our values of 2.80 eV for  $\text{PuO}_2$  and 2.85 eV for  $\text{NpO}_2$  based on optical band gap measurements values are consistent with the olive green color of the bulk oxides. Any material with a band gap as low as 1.8 eV (680 nm) or 0.4 eV (3100 nm) would be expected to

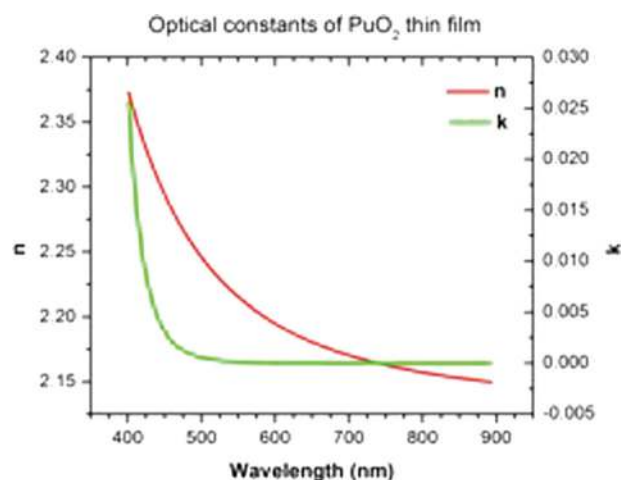


FIG. 5. Optical constants for  $\text{PuO}_2$ ; n (red) and k (green).

appear black at any reasonable crystallite size. In addition, we have been able to obtain the real and imaginary optical constants of the refractive index as a function of wavelength using ellipsometry with values of  $n=2.1$  and  $k=0.012$  at 500 nm (Figure 5).

The results reported here offer a new benchmark for theoretical calculations. Experimentally, we now have a way to measure both band gap and other optical properties on the same sample in order to determine the most accurate theoretical models and push them toward the realm of predictive value. The screened hybrid DFT approximation J. Heyd, G. E. Scuseria, and M. Ernzerhof (HSE) yields gaps of 3.1 eV and 2.7 eV for  $\text{NpO}_2$  and  $\text{PuO}_2$ ,<sup>29</sup> in excellent agreement with our measurements of 2.85 and 2.80 eV, respectively. The hybrid DFT calculations were spin polarized (unrestricted) and found an antiferromagnetic coupling solution as the ground state. These early HSE results did not examine the influence of spin-orbit coupling on the computed band gaps, but recent work using an approach identical to that in Peralta *et al.*<sup>30</sup> finds its influence to be minimal; inclusion of spin-orbit coupling within HSE yields 2.99 and 2.58 eV, respectively. A GGA + U calculation, specifically PBE + U,  $U=4.0$  eV, finds values of 2.6 and 1.6 eV for the band gaps of  $\text{NpO}_2$  and  $\text{PuO}_2$ ; the value for  $\text{PuO}_2$  somewhat lower than our experimental result.<sup>31</sup> The SIC approximation yields 2.3 eV and 1.2 eV,<sup>3</sup> respectively, again somewhat lower than experiment for  $\text{PuO}_2$ . To our knowledge, the gap for  $\text{NpO}_2$  from DMFT has not been reported, but for  $\text{PuO}_2$  the DMFT result depends upon the value chosen for the parameter U. DMFT yields either 3.5 eV ( $U=6$  eV)<sup>5</sup> or 2.5 eV ( $U=3$  eV) for the gap in  $\text{PuO}_2$ .<sup>6</sup> It is interesting and important that these various approximations also differ in other significant properties of the materials,<sup>31</sup> such as the character of the gap; that is, metal to metal versus ligand to metal charge transfer. Predictions about properties such as the magnetic ground states of these materials become very complicated as some energetic changes can have pronounced effects.  $\text{UO}_2$  is antiferromagnetic, the ordering of  $\text{NpO}_2$  is still controversial, and  $\text{PuO}_2$  has a nonmagnetic singlet ground state. None of the theories discussed here get the correct magnetic ground state in these three materials. The magnetic properties are



characterized by energy scales of the order of meV, as opposed to the band gaps which are of the order of several eV. The availability of fundamental experimental data on bandgaps provides a key first step in advancing f-element theories and needs to be followed by experimental work such as angle-resolved photoemission spectroscopy (ARPES) to assess dispersion of the bands and further theoretical advances to tackle the finer challenges of properties such as magnetism. We are currently in the process of measuring ARPES and other optical constants on these thin films to further constrain fundamental electronic structure approximations.

## EXPERIMENTAL METHODS

The precursor solution for making the PuO<sub>2</sub> films was prepared by binding a plutonium EDTA complex to PEI. In detail, a base solution of EDTA and PEI was prepared by adding EDTA (Aldrich 99.995%) to water purified to 18 Ω using a Milli-Q water treatment system followed by PEI purchased from BASF Corporation of Clifton, NJ (used without further purification). The pH of this solution was adjusted to 7, using concentrated hydrochloric acid. A stock solution of <sup>239</sup>Pu was of high purity containing 99.97% Pu with 23 ppm Am, 47 ppm Np, and an isotopic distribution based on weight % of 0.012 <sup>238</sup>Pu, 93.933 <sup>239</sup>Pu, 5.900 <sup>240</sup>Pu, 0.110 <sup>241</sup>Pu and 0.045 <sup>242</sup> Pu. Coating solutions were made from the base EDTA/PEI solution by adding 0.250 ml of PEI/EDTA and 0.140 ml of Pu stock solution to a vial and mixing. The neptunium precursor solution was prepared in the same manner, using a stock solution of <sup>237</sup>Np. The <sup>237</sup>Np concentration of the stock solution was 0.228 mol l<sup>-1</sup> in 3 M HNO<sub>3</sub>. Coating solutions were made from the base EDTA/PEI solution by adding 0.125 ml of PEI/EDTA and 0.056 ml of Np stock solution to a vial and mixing. The resulting coating solutions contained 3.02 mg of <sup>237</sup>Np and 3.84 mg of <sup>239</sup>Pu. No further purification was performed on the coating solution. The coating solutions were subsequently spin coated onto different substrates using a spin coater (Kemat Technology Spincoater, KW-4 A). Approximately, 0.025 ml of the coating solutions were applied to the substrate and spun at 3000 rpm for 30 s. The substrates were removed and annealed in air up to 1000 °C for 3 h by ramping to 120 °C at 1 °C/min; holding for 1 h; ramping to 350 °C at 1 °C/min; holding for 1 h; ramping to 100 °C at 1 °C/min; holding for 3 h and then cooling to room temperature.

X-ray diffraction measurements were made on a Bruker D8 Discover, with monochromatic CuK<sub>α</sub> radiation, and either a NiI scintillation or multi-wire gas proportional detector. Band gap measurements were made by measuring absorbance of two PuO<sub>2</sub> films, one with 3 coats of PuO<sub>2</sub> and one with 5 coats of PuO<sub>2</sub> on double sided polish YSZ (from MTI Corporation). Likewise, NpO<sub>2</sub> films were measured for absorbance. As a standard check, Fe<sub>2</sub>O<sub>3</sub> was deposited by the PAD process on c-cut sapphire and the measured band gap determined to be 2.25 eV ± 0.05 eV as previously reported in literature.<sup>32</sup> Absorbance of the films was taken on a Varian Cary 6000i UV-Vis-NIR spectrometer. Spectroscopic ellipsometry measurements over the wavelength range of 380–900 nm were performed using a J. A. Woollam alpha-SE, and

the data fit using a Cauchy function. Two PuO<sub>2</sub> films of differing thicknesses were used to iteratively adjust the fit to obtain consistent optical functions independent of the film thickness. The Pu L3 XAFS was measured and analyzed in fluorescence mode on beam line 11-2 at SSRL using 25 elements of a multi-element Ge detector and standard procedures including the energy calibration values reported previously by our group.<sup>33,34</sup>

## CONCLUSIONS

High quality epitaxial thin films of PuO<sub>2</sub> and NpO<sub>2</sub>, approaching single crystal quality, were synthesized using the solution method of polymer assisted deposition. XANES data show the PuO<sub>2</sub> films were essentially free of Pu(III) contamination, and EXAFS data suggest a degree of structural ordering that is possibly higher than single phase powders. The direct band gaps of these two actinide dioxides were measured for the first time, and gave values of 2.85 eV and 2.80 eV for PuO<sub>2</sub> and NpO<sub>2</sub>, respectively. These results are in excellent agreement with our previously reported numbers using screened hybrid DFT approximation (HSE); 3.1 and 2.7 eV.<sup>29</sup> These results have relevance in the understanding of nuclear fuel science and technology, as well as the fundamental understanding of f-orbital electron behavior. Future work will include the synthesis and study of films of mixed metal (Pu/U) oxide compositions relevant to MOX fuels.

## ACKNOWLEDGMENTS

This work at Los Alamos National Laboratory (LANL) was supported by the Laboratory Directed Research and Development program at LANL. The work at Rice University was supported by DOE Grant No. DE-FG02-04ER15523 (Heavy Element Chemistry Program at BES).

<sup>1</sup>I. D. Prodan, G. E. Scuseria, and R. L. Martin, "Assessment of metageneralized gradient approximation and screened Coulomb hybrid density functionals on bulk actinide oxides," *Phys. Rev. B* **73**, 045104 (2006).

<sup>2</sup>K. N. Kudin, G. E. Scuseria, and R. L. Martin, "Hybrid density-functional theory and the insulating gap of UO<sub>2</sub>," *Phys. Rev. Lett.* **89**, 266402 (2002).

<sup>3</sup>L. Petit, A. Svane, Z. Szotek, W. M. Temmerman, and G. M. Stocks, "Electronic structure and ionicity of actinide oxides from first principles," *Phys. Rev. B* **81**, 045108 (2010).

<sup>4</sup>V. I. Anisimov and A. I. Lichtenstein, *Strong Coulomb Interactions in Electronic Structure Calculations LDA + U Method: Screened Coulomb Interaction in the Mean-field Approximation* (Gordon and Breach Science, Amsterdam, 2000), Chap. 2.

<sup>5</sup>Q. Yin *et al.*, "Electronic correlation and transport properties of nuclear fuel materials," e-print arXiv:1012.2412v2.

<sup>6</sup>Q. Yin and S. Y. Savrasov, "Origin of low thermal conductivity in nuclear fuels," *Phys. Rev. Lett.* **100**, 225504-1-4 (2008).

<sup>7</sup>C. B. Finch and G. W. Clark, "High-temperature solution growth of single-crystal plutonium dioxide," *J. Cryst. Growth* **12**, 181–182 (1972).

<sup>8</sup>A. Modin *et al.*, "Indication of single-crystal PuO<sub>2</sub> oxidation from O 1s x-ray absorption spectra," *Phys. Rev. B* **83**, 075113 (2011).

<sup>9</sup>A. Modin *et al.*, "Closed source experimental system for soft x-ray spectroscopy of radioactive materials," *Rev. Sci. Instrum.* **79**, 093103 (2008).

<sup>10</sup>C. E. McNeilly, "The electrical properties of plutonium oxides," *J. Nucl. Mater.* **11**, 53–58 (1964).

<sup>11</sup>K. E. Roberts *et al.*, "Precipitation of crystalline neptunium dioxide from near-neutral aqueous solution," *Radiochim. Acta* **91**, 87–92 (2003).

<sup>12</sup>C. B. Finch and G. W. Clark, "High-temperature solution growth of single-crystal neptunium dioxide," *J. Cryst. Growth* **6**, 245–248 (1970).

- <sup>13</sup>J. C. Spirlet, W. Muller, and J. Van Audenhove, *Nucl. Instrum. Methods Phys. Res. A* **236**, 489–492 (1985).
- <sup>14</sup>P. Erdos, G. Solt, Z. Zolnieriek, A. Blaise, and J. M. Fournier, “Magnetic susceptibility and the phase transformation of  $\text{NpO}_2$ ,” *Physica B + C* **102**, 164–170 (1980).
- <sup>15</sup>A. K. Burrell, T. M. McCleskey, and Q. X. Jia, “Polymer assisted deposition,” *Chem. Commun.* **0**, 1271–1277 (2008).
- <sup>16</sup>Q. X. Jia *et al.*, “Polymer-assisted deposition of metal-oxide films,” *Nature Mater.* **3**, 529–532 (2004).
- <sup>17</sup>M. N. Ali, M. A. Garcia, T. Parsons-Moss, and H. Nitsche, “Polymer-assisted deposition of homogeneous metal oxide films to produce nuclear targets,” *Nat. Protoc.* **5**, 1440–1446 (2010).
- <sup>18</sup>H. Boukhalfa, S. D. Reilly, W. H. Smith, and M. P. Neu, “EDTA and mixed-ligand complexes of tetravalent and trivalent plutonium,” *Inorg. Chem.* **43**, 5816–5823 (2004).
- <sup>19</sup>L. Rao, G. Tian, and S. J. Teat, “Complexation of  $\text{Np(V)}$  with  $\text{N,N}$ -dimethyl-3-oxa-glutaramic acid and related ligands: thermodynamics, optical properties and structural aspects,” *Dalton Trans.* **39**, 3326–3330 (2010).
- <sup>20</sup>A. K. Burrell *et al.*, “Controlling oxidation states in uranium oxides through epitaxial stabilization,” *Adv. Mater.* **19**, 3559–3563 (2007).
- <sup>21</sup>H. Luo *et al.*, “Controlling crystal structure and oxidation state in molybdenum nitrides through epitaxial stabilization,” *J. Phys. Chem. C* **115**, 17880–17883 (2011).
- <sup>22</sup>K. Richter and C. Sari, “Phase relationships in the neptunium-oxygen system,” *J. Nucl. Mater.* **148**, 266–271 (1987).
- <sup>23</sup>E. R. Gardner, T. L. Markin, and R. S. Street, “The plutonium-oxygen phase diagram,” *J. Inorg. Nucl. Chem.* **27**, 541–551 (1965).
- <sup>24</sup>J. M. Hashke, T. H. Allen, and L. A. Morales, “Reaction of plutonium dioxide with water: formation and properties of  $\text{PuO}_{2+x}$ ,” *Science* **287**, 285–287 (2000).
- <sup>25</sup>A. Seibert, T. Gouder, and F. Huber, “Reaction of neptunium with molecular and atomic oxygen: formation and stability of surface oxides,” *J. Nucl. Mater.* **389**, 470–478 (2009).
- <sup>26</sup>S. D. Conradson *et al.*, “Higher order speciation effects on plutonium L-3 X-ray absorption near edge spectra,” *Inorg. Chem.* **43**, 116–131 (2004).
- <sup>27</sup>J. Schoenes, “Optical properties and electronic structure of  $\text{UO}_2$ ,” *J. Appl. Phys.* **49**, 1463–1465 (1978).
- <sup>28</sup>S. R. Gosavi, N. G. Deshpande, Y. G. Gudage, and R. Sharma, “Physical, optical and electronic properties of copper selenide ( $\text{CuSe}$ ) thin films deposited by solution growth technique at room temperature,” *J. Alloys Compd.* **448**, 344–348 (2008).
- <sup>29</sup>I. D. Prodan, G. E. Scuseria, and R. L. Martin, “Covalency in the actinide dioxides: Systematic study of the electronic properties using screened hybrid density functional theory,” *Phys. Rev. B* **76**, 033101 (2007).
- <sup>30</sup>J. E. Peralta, J. Heyd, G. E. Scuseria, and R. L. Martin, “Spin-orbit splittings and energy band gaps calculated with the Heyd-Scuseria-Ernzerhof screened hybrid functional,” *Phys. Rev. B* **74**, 073101 (2006).
- <sup>31</sup>X. D. Wen *et al.*, “Effect of Spin-orbit coupling on the actinide dioxides  $\text{AnO}_2$  ( $\text{An} = \text{Th}, \text{Pa}, \text{U}, \text{Np}, \text{Pu}$  and  $\text{Am}$ ): A screened hybrid density functional study,” *J. Chem. Phys.* **137**, 154707 (2012).
- <sup>32</sup>K. Kaneko, T. Nomura, K. Kakeya, and S. Fujita, “Fabrication of highly crystalline corundum-structured  $\alpha$ - $(\text{GA}_{1-x}\text{Fe}_x)_2\text{O}_3$  alloy thin films on sapphire substrates,” *Appl. Phys. Express* **2**, 075501 (2009).
- <sup>33</sup>S. D. Conradson *et al.*, “Local and nanoscale structure and speciation in the  $\text{PuO}_{2+x-y}(\text{OH})_{2y} \cdot z\text{H}_2\text{O}$  system,” *J. Am. Chem. Soc.* **126**, 13443–13458 (2004).
- <sup>34</sup>See supplementary material at <http://dx.doi.org/10.1063/1.4772595> for plot of optical band gap for  $\text{NpO}_2$ .